Environmental Science: Atmospheres

ROYAL SOCIETY OF CHEMISTRY

PAPER

View Article Online
View Journal | View Issue

Cite this: *Environ. Sci.: Atmos.*, 2024, **4**, 1239

Immersion ice nucleation of atmospherically relevant lipid particles†

Lincoln Mehndiratta, Audrey E. Lyp, Jonathan H. Slade * and Vicki H. Grassian *

Received 24th May 2024
Accepted 25th September 2024

DOI: 10.1039/d4ea00066h

rsc.li/esatmospheres

Ice nucleating particles (INPs) play a crucial role in freezing water droplets by acting as heterogeneous ice nuclei, influencing cloud phase state and climate dynamics. INPs from marine aerosol particles are particularly relevant. Saturated fatty alcohols and acids have been identified in sea spray aerosols (SSA). In this study, we employ a micro-Raman spectrometer integrated with an environmental cell to control relative humidity and temperature and measure the ice nucleation activity of individual lipid particles, including fatty alcohols and fatty acids of varying chain lengths. For fatty acids, we observe little IN activity for these lipid particles as they freeze close to the temperature found for homogeneous freezing. For fatty alcohols, we demonstrate that freezing temperatures depend on the carbon chain length, with longer chains leading to warmer ice nucleating temperatures. Although this result qualitatively agrees with existing literature, we observe that the ice nucleating temperatures of these lipid particles differ from the freezing temperatures measured for fatty alcohol monolayers at the air/water interface for large water droplets. To better understand these differences, we further investigate the effects of droplet size as well as phase state by theoretically determining the wet viscosity on freezing. Our results, taken together, suggest that for fatty alcohol particles, freezing occurs at the lipid particle/water interface. Overall, our findings highlight the influence of lipid chain length, droplet size, and phase state on ice nucleation for lipid particles.

Environmental significance

Ice particles are essential for cloud formation, precipitation, and influencing the Earth's radiative balance. Oceans, covering nearly three-quarters of the Earth's surface, produce sea spray aerosols (SSA) that serve as significant ice nucleating particles (INPs). Despite their importance, the ice nucleation ability of key organic carbon species in SSA, such as fatty alcohols and fatty acids, need to be further understood. We measured ice nucleation temperatures of droplets containing marine-relevant lipid particles, including fatty alcohols and fatty acids. Our results reveal that droplet size, lipid chain length, and lipid phase state (liquid, semisolid, or solid) can impact ice nucleation.

Introduction

Around 67% of Earth's surface is covered by clouds, which influence the Earth's radiative budget and climate system through the changes in cloud albedo, precipitation, cloud coverage, and lifetime.[1,2] Ice clouds (consisting of ice crystals) and mixed-phase clouds (comprising ice crystals and water droplets) are prevalent in the upper atmosphere at higher altitudes, particularly in regions characterized by colder temperatures within the Earth's atmosphere.[1] The presence of aerosol particles, their composition, water content, and air temperature can affect the microphysical properties of these clouds.[1] The formation of ice crystals within both ice-phase and mixed-phase clouds is facilitated by ice nucleating particles (INPs).[1] INPs are a distinctive subgroup of aerosols, which can still have a significant impact on cold cloud microphysical processes despite their low concentrations, sourced from a diverse range of origins and compositions, such as dust, minerals, combustion byproducts, and SSA.[3–6] Only one in 10^5 to 10^6 atmospheric aerosol particles can act as INPs.[7] The creation of ice and mixed-phase clouds are directly influenced by alterations in ice nucleation pathways, subsequently affecting precipitation,

Department of Chemistry & Biochemistry, University of California San Diego, 9500 Gilman Dr, La Jolla, California 92093, USA. E-mail: vhgrassian@ucsd.edu; jhslade@ucsd.edu

† Electronic supplementary information (ESI) available: Supporting information contains four figures and a table, which include a figure of the calibration curve of the environmental cell between the set and sample temperature, a table of ice nucleation weighted mean average temperatures of fatty acids and fatty alcohols along with their standard deviation, a figure between weighted mean ice nucleation temperature (with standard deviation) and 50% ice nucleation temperature for the lipids, milliQ water, Snomax and NaCl, a figure showing a correlation plot between weighted mean ice nucleation temperature and 50% ice nucleation temperature for the fatty acids, and a figure between ice nucleation temperature and log wet viscosities for fatty acids, and a correlation plot between them. See DOI: https://doi.org/10.1039/d4ea00066h

cloud coverage, and optical depth.[1,8,9] Owing to this intricate nature, the aerosol components involved in aerosol–cloud interactions continue to pose one of the most significant uncertainties in climate models.[10] While considerable research has been conducted on ice nucleation, ongoing efforts are being made to discern the chemical and physical characteristics that govern the activity of marine and biologically relevant ice-nucleating particles.[11–16] Specifically, an ongoing endeavor to identify the ice-nucleating particles originating from marine organisms that have the most significant impact on cloud formation in distant marine areas.[3,17,18]

Ice formation in the earth's atmosphere occurs broadly *via* homogeneous and heterogeneous freezing processes. Homogenous ice nucleation occurs when a water droplet is supercooled below −38 °C, and ice crystals are formed without foreign particles. Heterogeneous ice nucleation involves foreign entities with surfaces that can facilitate the freezing of water droplets into ice crystals at warmer temperatures.[19] Heterogeneous ice nucleation can mainly occur through two pathways: deposition freezing and immersion freezing. Deposition freezing, crucial in forming ice clouds, occurs when humidity increases, subsequent to a decrease in temperature.[20] Immersion freezing initiates with an initial rise in relative humidity (RH), resulting in water condensation, followed by a temperature decrease, inducing the formation of a supercooled droplet and eventually undergoing a phase transition to form ice, as shown in Fig. 1. Immersion freezing is a crucial factor in forming mixed-phase clouds, wherein ice-nucleating particles are anticipated to prompt droplet formation before freezing occurs.[4–6,21–25]

The Earth's surface is predominantly covered by oceans, particularly in the Southern Hemisphere, where INPs exert the greatest influence.[3,4,17,18,26–28] At the boundary between the atmosphere and the ocean, primary SSA is created as bubbles from breaking waves burst.[14,29,30] SSA represents the major annual contributor of aerosol flux by mass into the atmosphere.[10,31–33] Additionally, SSA is recognized as a significant source of INPs. The significance of SSA particles in forming atmospheric ice clouds is thoroughly documented.[3,15,18,30,34–38] Modeling results indicate that biogenic organic matter exerts a worldwide influence on forming atmospheric ice clouds through immersion ice nucleation.[3,4,15] There is also direct evidence from mesocosm studies indicating that atmospheric INPs originate from organic material.[17,37,39] To enhance our comprehension of the radiative impacts of primary SSA particles, it is important to investigate their chemical and physical attributes and INP potential. With this objective in sight, several studies have focused on delineating the chemical composition of overall aerosols across diverse marine settings.[31–33,40–42]

Primary SSA comprises a blend of inorganic salts, particulate biological elements such as intact bacteria and viruses, and organic matter.[14,31,43,44] Field investigations indicate that the predominant organic matter content in sub-micrometer aerosols is water-insoluble mainly, while in larger super-micrometer aerosols, it is predominantly water-soluble.[7,40,45–50] Field-collected SSA particles subjected to spectroscopic measurements have revealed that the oxygen-rich organic segment of these particles contains molecules displaying spectral characteristics typical of saccharides.[51,52] Additionally, signatures indicative of carboxylic acids and alkanes have also been identified.[47,52,53] Cochran *et al.*[52] employed micro-Raman spectroscopy to analyze the vibrational spectra of individual SSA particles freshly produced through wave breaking in controlled ocean-like conditions within a wave flume. They identified long-chain saturated fatty acids (C_{12}–C_{18}) and short-chain saturated fatty acid (C_5–C_{10}) particle types within SSA samples. Fatty acids and fatty alcohols are recognized as products of the biogenic degradation of cell membranes. Fatty alcohols have been detected both in the sea surface microlayer[54,55] and in marine aerosols across remote areas, likely originating from terrestrial sources that also contribute particles to the ocean surface.[56,57]

Most of the research on the freezing efficiency of fatty alcohols and acids has examined monolayers within large water droplets, typically around 1000 μm or larger. In this study, our focus lies in the immersion ice nucleation of individual substrate-deposited micron-sized lipid particles composed of either fatty alcohols (nonanol, decanol, dodecanol, tetradecanol, hexadecanol and octadecanol) or fatty acids (nonanoic acid, dodecanoic acid, hexadecanoic acid and octadecanoic acid), using confocal Raman spectroscopy. Furthermore, the physicochemical properties of the lipid particles, such as viscosity, may alter ice nucleation ability by affecting the extent to which the particles participate in heterogeneous freezing processes. For example, particles with glassy or solid-like phase states participate in homogeneous and heterogeneous freezing processes, freezing more efficiently (*i.e.*, at warmer temperatures) than liquid particles.[58–62] Overall, this study endeavors to understand the impact of lipid molecular size (chain length), particle size, water solubility, and viscosity at the freezing temperature on the ice-nucleating ability of marine-type particles.

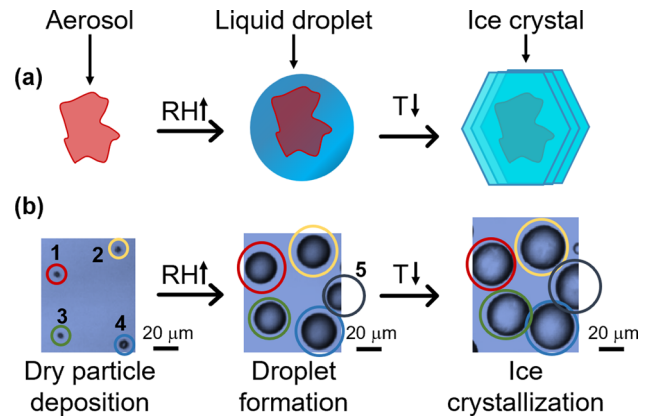

Fig. 1 (a) Conceptual schematic diagram depicting immersion ice nucleation in the atmosphere. (b) Microscopy images including scale bars, illustrating the stages of immersion ice nucleation from one experiment, including dry deposited particles (particle 1 = 3.1 μm, particle 2 = 4.7 μm, particle 3 = 3.8 μm, particle 4 = 7.9 μm), formation of wet droplets by increasing relative humidity, and ice crystal formation by decreasing the temperature. Particle 5 was initially not observed, as it was smaller than the resolution of the 10× objective. However, it appears in the image when the larger droplet forms and then when it becomes ice.

Materials and methods

Materials, chemicals, and sample preparation

All chemicals were purchased directly from manufacturers and used without further purification. Chemicals include sodium chloride (NaCl, ≥99%, Fisher Scientific) and *Pseudomonas syringae* (Snomax, York Snow Inc.) to show examples of freezing depression and efficient nucleation, respectively. Snomax is a commercially available product derived from the bacterium *Pseudomonas syringae*. Other compounds include nonanol ($C_9H_{19}OH$, 98%, Sigma-Aldrich), decanol ($C_{10}H_{21}OH$, 98+%, Alfa Aesar), dodecanol ($C_{12}H_{25}OH$, >99.0%, TCI Chemicals), tetradecanol ($C_{14}H_{29}OH$, >98.0%, TCI Chemicals), hexadecanol ($C_{16}H_{33}OH$, 99%, Sigma-Aldrich), octadecanol ($C_{18}H_{37}OH$, 99%, Sigma-Aldrich), nonanoic acid ($C_8H_{17}COOH$, 96%, Sigma-Aldrich), dodecanoic acid ($C_{11}H_{23}COOH$, 99%, Thermo Scientific), hexadecanoic acid ($C_{15}H_{31}COOH$, ≥99%, Sigma-Aldrich) and octadecanoic acid ($C_{17}H_{35}COOH$, ≥98.5%,Sigma-Aldrich). Ethanol was used as the solvent in solution preparations except for sodium chloride, for which Milli-Q ultrapure water was used. Table S1 of the ESI† provides details of the physical state at 25 °C and the melting point of the fatty alcohols and fatty acids.

Methods

Calibration of the environmental cell

The environmental cell (Linkam, THMS600) was full calibrated to compensate for variations between the preset temperature and the temperature observed by the particles deposited on the substrates within the cell.[63–67] For example, using NaCl, known to have a deliquescence relative humidity (DRH) of 75% over a wide spectrum of temperatures,[68] was used to generate a calibration curve of the effective particle temperature,[63,64] which is different from the set point temperature. For each set temperature point, a fresh aerosolized NaCl sample was generated specifically for calibration. Before each experiment, the deposited samples underwent a 15 minutes calibration period within the cell, during which they were dried under N_2. Subsequently, there were gradual increments in relative humidity (RH), with 10 minutes equilibration periods separating each increase (RH increased from 0.3% to DRH of NaCl). Both visual and spectral examinations corroborated deliquescence, characterized by an expansion in particle size, observable darkening of the droplet under an optical microscope, and a sudden large increase in intensity in the O–H stretching region spanning 3000 to 3700 cm^{-1}. At the deliquescence point, temperature and dew point readings were recorded using a hygrometer to calculate the relative humidity (RH) in the environmental cell. The calibration of the environmental cell and the cooling rate's effects on pure water's ice nucleation temperature has been previously discussed and detailed by Mael *et al.*[64–67] Fig. S1† shows the calibration curve, illustrating its linearity within the range of temperatures from −45 to 23 °C.

Aerosol generation using a nebulizer

A mesh nebulizer (OMRON, NE-U22-E), which works on vibrating mesh technology, generated aerosolized lipid particles. This nebulizer has three parts: a power unit, a solution container, and a mesh cap. The solution container is the reservoir, and the mesh cap uses pores to make 1–5 μm aerosolized particles. Fatty alcohol and fatty acid solutions in ethanol were put into the medication container of the nebulizer, and the aerosol particles that formed (about 1–10 μm) were collected onto hydrophobic quartz substrates coated by Rain-X.

Ice nucleation measurements using confocal Raman spectroscopy

Freezing measurements were conducted using a Raman microscope (Horiba, LabRam HR Evolution) with a 532 nm laser coupled to an environmental cell as described previously in detail.[64,66] The spectrometer has an optical microscope (Olympus BX41) and a 100× super long working distance objective (SLWD). The environmental cell features gas inlets and an exhaust line linked to a hygrometer (Buck, CR-4) and a temperature controller, enabling precise regulation of temperature and relative humidity (RH). Lipid particles deposited onto a quartz substrate were placed in the environmental cell, and a dry N_2 flow was sent through the cell for 15 minutes. A Raman spectrum of the lipid particle was after following this 15 minutes N_2 purge. The RH was controlled by circulating N_2 through a bubbler filled with Milli-Q water and adjusting the proportion of moist to dry N_2 directed into the environmental cell. The relative humidity was increased until a water droplet formed above the lipid particle as evidenced by the Raman spectrum showing the presence of the broad peak due to the O–H stretch of liquid water. The temperature of the cell was then dropped (rate = −10 °C min^{-1}), and the droplets with the embedded lipid particles were observed to change from liquid water to ice as observed by changes in the optical image and in the O–H stretch in the Raman spectrum, as shown in Fig. 2. The spectrum displayed in Fig. 2(c) exhibits a broad O–H stretch peak with peak maxima and shoulders at 3133, 3260, and 3344 cm^{-1} wavenumbers. These frequencies correspond to hexagonal ice, indicating that the ice formed from these water droplets containing lipid particles is in the hexagonal ice structure.[69–71]

Calculation of ice nucleation weighted mean temperatures

As noted above, in a typical experiment, particles of fatty alcohols and fatty acids deposited on a hydrophobic substrate are then exposed to increasing relative humidity to form a water droplet, followed by decreasing temperature to form ice. In each experiment, approximately 30 to 70 substrate-deposited lipid particles were observed using a 10× microscope objective, utilized with the Raman spectrometer. Two to three independent ice nucleation experiments, which included 100 to 150 lipid particles, were conducted for each lipid to ensure reproducibility. A video recording followed the entire experiment from a lipid particle to an aqueous water droplet containing a lipid particle to an ice-containing lipid particle. The temperatures at which individual lipid particles induced ice formation were recorded to compute the ice nucleation weighted mean

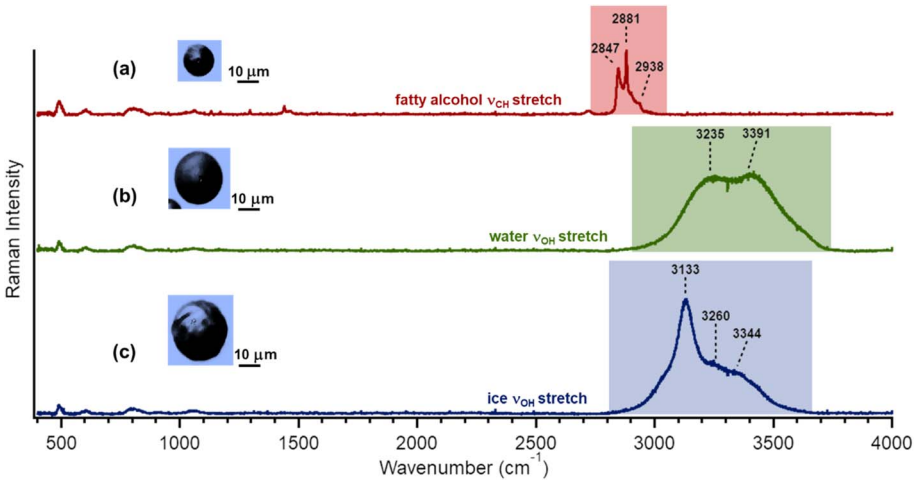

Fig. 2 Immersion freezing of substrate-deposited lipid particles utilizing micro-Raman spectroscopy. (a) Spectrum and an optical image of a ~10 μm diameter hexadecanol particle with peaks within the C–H stretching region at 2847, 2881, and 2938 cm^{-1}. (b) Spectrum after the relative humidity is raised to form a water droplet, with prominent broad peaks observed in the O–H stretching region at 3235 and 3391 cm^{-1}, indicating the presence of liquid water. (c) The same particle as in (a and b) at a lower temperature, where ice formation is evidenced by the O–H vibrational bands at 3133, 3260, and 3344 cm^{-1}. Vertical axis scales are different and have been magnified for the lipid particle compared to the droplet and ice spectrum.

average. Additionally, standard deviations were calculated to assess data variability.

Theoretical viscosity estimation derived from molecular composition

Each lipid particle phase state or viscosity (η) was estimated from the theoretical glass transition temperature of the organic–water mixture ($T_{g,org,wet}$), as done in previous studies, as shown in eqn (1)–(3).[72–75]

$$T_{g,org} = A + BM + CM^2 + D(O:C) + EM(O:C) \quad (1)$$

$$T_{g,org,wet} = \frac{(1 - w_{org})T_{g,w} + \frac{1}{k_{GT}} w_{org} T_{g,org}}{(1 - w_{org}) + \frac{1}{k_{GT}} w_{org}} \quad (2)$$

$$\log\eta = -5 + 0.434\left(\frac{T_0 D}{T - T_0}\right) \quad (3)$$

The model parameterizes the dry glass transition temperature ($T_{g,org}$) from the particle's molar mass (M) and oxygen-to-carbon (O : C) ratio, where $A = -21.57$ (± 13.47) [K], $B = 1.51$ (± 0.14) [K mol g^{-1}], $C = -1.7 \times 10^{-3}$ ($\pm 3.0 \times 10^{-4}$) [K mol^2 g^{-2}], $D = 131.4$ (± 16.01) [K], $E = -0.25$ (± 0.085) [K mol g^{-1}] are fitting constants. $T_{g,org,wet}$ was parameterized from $T_{g,org}$ using the Gordon–Taylor equation (eqn (2)), where w_{org} is the mass fraction of organics as $w_{org} = m_{org}/(m_{org} + m_{H_2O})$, $T_{g,w}$ is the glass transition temperature of pure water (136 K), and k_{GT} is the Gordon–Taylor constant assumed to be 2.5 (± 1.0). T_0 is the Vogel temperature, and T is the ambient temperature.

The mass of water (m_{H_2O}) in the particles was estimated using the effective hygroscopicity parameter (κ_i), where i represents the individual organic components. The water activity was assumed to be RH = 80%. Since this value for fatty alcohols and fatty acids is unknown, we rely on the approach of Mikhailov *et al.*[76] to estimate the κ_i of these organic compounds using eqn (4).

$$k_i = J_i \times \left(\frac{\frac{\rho_i}{M_i}}{\frac{\rho_w}{M_w}}\right) \quad (4)$$

where J_i represents the van't Hoff factor, ρ_i and M_i denote the density and molar mass of the solute (i) and water (w), respectively. J_i was assumed to be 1 for the studied molecules. By employing the model, we computed the η of the droplet upon deliquescence near its freezing temperature. This is represented as the "log η_{wet}," which represents the logarithm of a droplet's viscosity after its water uptake. Materials exhibiting $\eta_{wet} > 10^{12}$ Pa s ($\log \eta_{wet} > 12$) are classified as solid-like, while those with $\eta_{wet} = 10^2$–10^{12} Pa s ($2 < \log \eta_{wet} < 12$) are categorized as semi-solid, and those with $\eta_{wet} < 10^2$ Pa s ($\log \eta_{wet} < 2$) are liquid.[58]

Results and discussion

Weighted ice nucleation mean averages of fatty alcohols and fatty acids

Immersion ice nucleation measurements were conducted on individual micron-sized, supercooled droplets containing fatty alcohols (nonanol, decanol, dodecanol, tetradecanol, hexadecanol and octadecanol) and fatty acids (nonanoic acid, dodecanoic acid, hexadecanoic acid and octadecanoic acid). These fatty alcohols and fatty acids were selected to investigate their ice nucleation characteristics as they are atmospherically relevant marine compounds.[52,54–57] Additionally, Snomax, Milli-Q water, and NaCl were included as standard references for immersion freezing behavior. As discussed, each ice nucleation

experiment involved depositing a lipid particle, which was then exposed to increasing relative humidity (RH) within the environmental cell and then decreasing temperature. Furthermore, this transition was tracked using Raman spectroscopy, wherein the growth in the band associated with the O–H stretching motion (ν(OH)) from 3000 to 3700 cm^{-1} was monitored. Subsequently, the cell's temperature was reduced (rate = −10 °C min^{-1}), and the particles were monitored until the transition from droplet to ice occurred. Size and morphology changes were observed using an optical microscope, as shown in Fig. 2.

In previous studies, fatty alcohols were found to be effective ice nuclei when prepared as monolayers on very large droplets on the order of several hundreds of μm in size.[77–80] Differences in chain lengths were shown to result in different ice nucleation temperatures with increasing freezing temperature observed with an increase in hydrocarbon chain length.[77,78,81] Fatty alcohols have garnered considerable interest because they are among the few identified compounds capable of nucleating ice and are also prevalent in the environment. Ochshorn[82] *et al.* investigated the ability of fatty alcohols to act as templates for ice formation and facilitate freezing. Theoretical studies by Qiu *et al.*[83] showed that monolayers of fatty alcohols at the air/water interface result in the fatty alcohol hydroxyl groups arranged to resemble the structure found in the basal plane of ice. It has been suggested that matching lattices between ice and the surface governs their efficiency in nucleating ice.[83] In addition, organic monolayers are characterized by their soft nature and exhibit notable fluctuations.[83] It has also been hypothesized that these fluctuations contribute to the nucleation of ice.[83] In other studies, a "refreezing" phenomenon in fatty alcohol films were observed, whereby films displayed enhanced ice nucleation ability after being frozen and thawed. This effect seemed to diminish if the film was allowed to warm adequately between cycles. They postulated that the phenomenon stemmed from alterations in the structure of the monolayer film.[79,84] Fatty acid monolayers, on the other hand, have been shown to exhibit poor IN capabilities.[2]

Fig. 3 shows weighted mean ice nucleation temperatures of fatty alcohol and fatty acid particles embedded in water droplets compared with pure water droplets (homogeneous ice nucleation), NaCl droplets (freezing point depression and poor heterogeneous ice nuclei), and Snomax (good heterogeneous ice nuclei). Weighted mean IN temperatures and standard deviations for the fatty alcohol and fatty acid particles are tabulated in Table S1.† These results show that fatty alcohol particles serve as effective ice nuclei, with their IN temperatures demonstrating a chain length-dependent behavior, in line with earlier reports,[77] although quantitatively different. Specifically, we observed longer chain-length fatty alcohol particles exhibited greater nucleating ice efficiency than shorter chain lengths. Gavish *et al.*[77] observed fatty alcohol monolayers were nucleating ice in the range of −14 to −8 °C for carbon chain length between C_{14} and C_{30}. Here, we show for lipid particles that the freezing temperatures of hexadecanol and octadecanol were approximately 8 to 10 °C lower than that reported earlier.[77] Perkins *et al.*[85] also looked at the freezing efficiency of C_{16} and

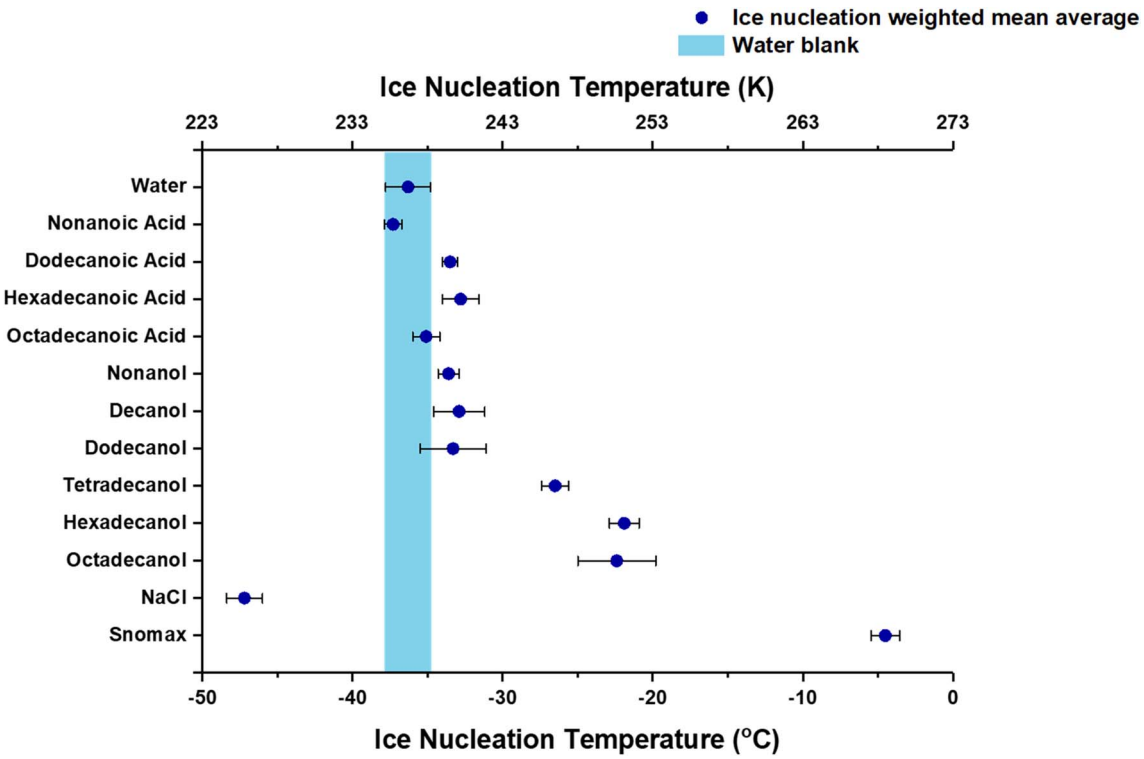

Fig. 3 Ice nucleation weighted mean average temperatures are indicated by blue circles, with their respective uncertainties for lipid particles, both fatty alcohols and fatty acids, along with Snomax and NaCl. The blue box depicts the freezing temperature of the water blank and the uncertainty in the measurement.

C_{18} fatty acids and fatty alcohols. They mixed fatty acids and fatty alcohols, adjusting their ratio within the monolayer, and subsequently measured the freezing efficiency. For the pure monolayer of C_{18} alcohol, they found the freezing temperature between −16 to −21 °C based on the amount of material deposited per molecule. For pure monolayer of C_{16} alcohol, the freezing temperature was −14.8 °C. The variance between this current study and earlier ones can be attributed to several factors, including the use of lipid particles compared to lipid monolayers. Additionally, this current study broadens our investigation to encompass shorter-chain fatty alcohols, namely nonanol, decanol, and dodecanol. Our observations indicate that these compounds nucleate ice albeit close to but above the homogeneous ice nucleation temperature of approximately −38 °C.[86–90]

Using nonanoic acid, dodecanoic acid, hexadecanoic acid, and octadecanoic acid, the fatty acid particles differ from the fatty alcohol particle analogs. Our observations indicate that two fatty acids (dodecanoic and hexadecanoic acid) nucleate ice outside (at a warmer temperature) of the homogeneous freezing temperature of water. In contrast, the others are within the range found for homogeneous ice nucleation.

Understanding the behavior of fatty acid particles is crucial, as demonstrated by McCluskey *et al.*'s[37] study, where long-chain fatty acids comprised approximately 18% of particles within the submicron diameter range in their plunging water mesocosm experiment. We conducted measurements of the 50% frozen values for both fatty alcohols and fatty acids, as shown in Fig. S2.† These values represent the points at which 50% of the observed population of fatty alcohol or fatty acid particles nucleated ice (*vide infra*). Our observed 50% frozen values closely paralleled the weighted mean average IN temperatures, with a correlation factor of 0.99, as depicted in Fig. S3.† Our findings align with previous literature studies,[2] which indicated that the freezing range for 50% of droplets composed of lipid particles with chain lengths of C_{12}, C_{14}, C_{16}, and C_{18} acids fell between −33 °C and −37 °C.

Frozen fraction curves of fatty alcohol and fatty acid particles

We quantified frozen fraction, eqn (5), defined as the proportion of particles that underwent ice formation at a specified temperature across the entire particle population. To analyze this, we segmented temperature ranges into bins of 1 °C increments and sorted particles into respective bins based on their freezing temperatures.

$$\text{Frozen fraction} = \frac{N_f(T)}{N_0} \quad (5)$$

where $N_f(T)$ is the number of frozen particles observed at the temperature T, and N_0 is the total number of droplets.

We generated frozen fraction curves to gain deeper insights into the freezing behavior of fatty alcohols and fatty acids, as shown in Fig. 4. These curves illustrate the correlation between the frozen fraction, representing the proportion of particles that have undergone freezing, and the corresponding temperature at which freezing occurs. This relationship provides valuable insights into the freezing behavior of fatty alcohol and fatty acid particles.

As previously noted, longer chain-length fatty alcohols are better ice nuclei than shorter ones. Fig. 4 illustrates the frozen fraction curves of the fatty alcohols. It is evident from the figure that fatty alcohol particles with longer chain lengths, such as hexadecanol (C_{16}) and octadecanol (C_{18}), exhibit frozen fraction curves shifted to the right (at warmer temperatures, making them better ice nuclei) compared to those with shorter chain lengths like nonanol (C_9), decanol (C_{10}), and dodecanol (C_{12}), whereas tetradecanol (C_{14}) falls in between. Most fatty alcohol particles exhibit distinct frozen fraction curves, characterized by a sharp transition where a significant portion of particles nucleate ice within a narrow temperature range. However, decanol, dodecanol, and octadecanol display a tail at warmer temperatures. To better understand this tail, we analyzed the different-sized droplets used for this study, as discussed below.

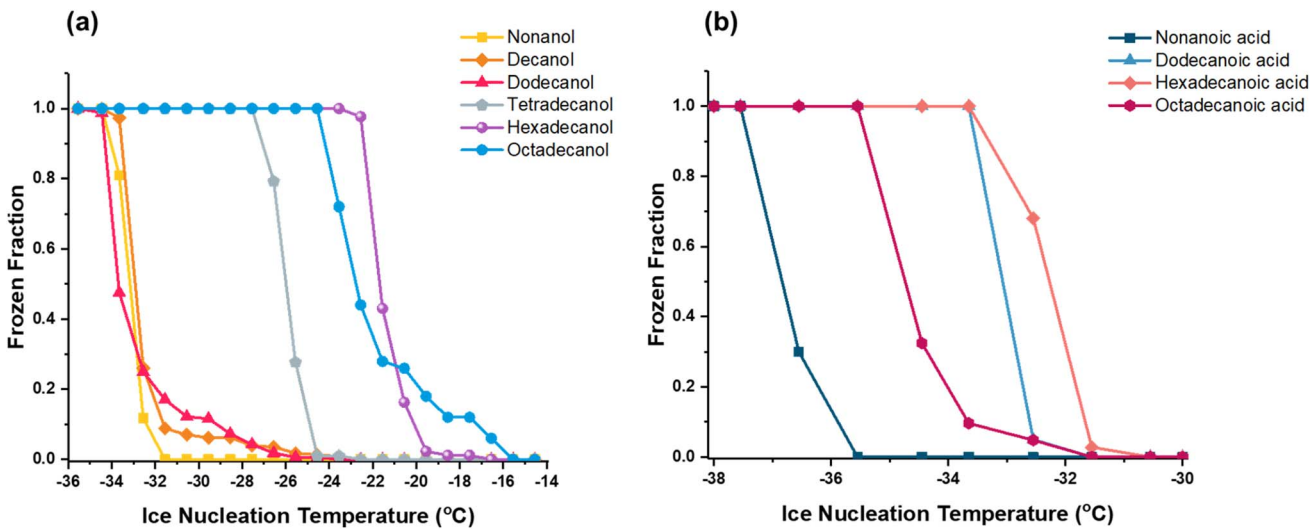

Fig. 4 The frozen fraction of (a) fatty alcohols and (b) fatty acids relative to the temperature at which the individual droplets underwent freezing.

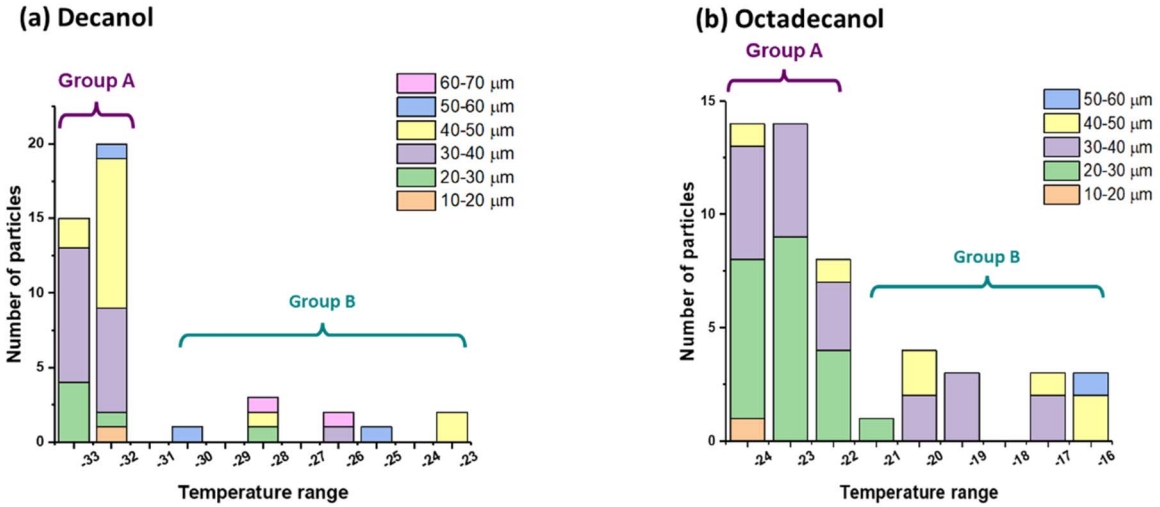

	Temperature (°C)	% of particles	
		Below 50 μm	Above 50 μm
Group A	-34 < T < -32	87.2	20
Group B	-32 < T < -23	12.8	80

	Temperature (°C)	% of particles	
		Below 40 μm	Above 40 μm
Group A	-25 < T < -22	81	25
Group B	-22 < T < -16	19	75

Fig. 5 (a) and (b) Represent the size analysis of immersion freezing experiments conducted on decanol and octadecanol, respectively. The size data has been categorized into Group A and Group B, representing the majority and minority populations for freezing. The table illustrates the percentage of droplets in larger and smaller sizes nucleating ice at colder and warmer temperatures, suggesting the larger droplets nucleate ice more readily.

Droplet size effects on freezing

Our frozen fraction curve analysis considers droplets within a range of droplet sizes (10–70 μm), as has been done for droplet size ranges in Murray *et al.*,[91] rather than individually due to the high variability in droplet size from the collection of polydisperse substrate-deposited particles. Including multiple-sized droplets in the analysis likely leads to uncertainty in the derived frozen fraction since supercooled freezing depends on volume. To better understand how size impacted the frozen fraction curve, Fig. 5 shows the number of frozen droplets within a narrower size range (increments of 10 μm) detected at a given freezing temperature. These results qualitatively indicate that lower temperatures are required to freeze the smallest particles, and the largest particles freeze at warmer temperatures.

A tail in the frozen fraction curves of decanol, dodecanol, and octadecanol may be attributed to the dependence of freezing temperature on droplet size. We reanalyzed the ice nucleation data of decanol and octadecanol to delve deeper into size effects. We measured the size of droplets nucleating ice and divided them into two groups, labeled Group A and Group B, as depicted in Fig. 5.

We constructed a histogram illustrating the count of droplets nucleating ice across various temperature ranges for different observed sizes for decanol and octadecanol. To investigate size dependence, we categorized the temperature ranges into two groups, Group A and Group B, where Group A was the temperature range where most of the droplets formed ice. The percentage of droplets nucleating ice below a specific size threshold was then examined. Decanol revealed that among smaller-sized droplets (below 50 μm), 87.2% nucleated ice in the colder temperature range (−34 °C < T < −32 °C), while only 12.8% nucleated into ice at warmer temperatures (−32 °C < T < −23 °C). Conversely, among larger-sized droplets (above 50 μm), only 20% nucleated ice in the colder temperature range (−34 °C < T < −32 °C), while 80% nucleated into ice at warmer temperatures (−32 °C < T < −23 °C). Octadecanol exhibited similar trends. Among smaller-sized droplets (below 40 μm), 81% nucleated ice in the colder temperature range (−25 °C < T < −22 °C), while only 19% nucleated into ice at warmer temperatures (−22 °C < T < −16 °C). Conversely, among larger-sized droplets (above 40 μm), only 25% nucleated ice in the colder temperature range (−25 °C < T < −22 °C), while 75% nucleated into ice at warmer temperatures (−22 °C < T < −16 °C). These findings indicate smaller droplets exhibit ice nucleation at colder temperatures, suggesting a potential correlation between droplet size and IN temperature.

Ice nucleation and viscosity

Several studies have explored the relationship between the phase state and homogeneous and deposition freezing. It has been shown for secondary organic material that a glassy or viscous phase state might be essential but not entirely indicative of ice nucleation in an organic particle.[92] In low-temperature cirrus environments, characterized by the presence of highly viscous organic aerosols in a glassy phase, evidence suggests that these particles may indeed nucleate ice, mainly through the deposition mode of freezing.[93] Murray *et al.*[94] demonstrated that glassy aerosol particles, such as citric

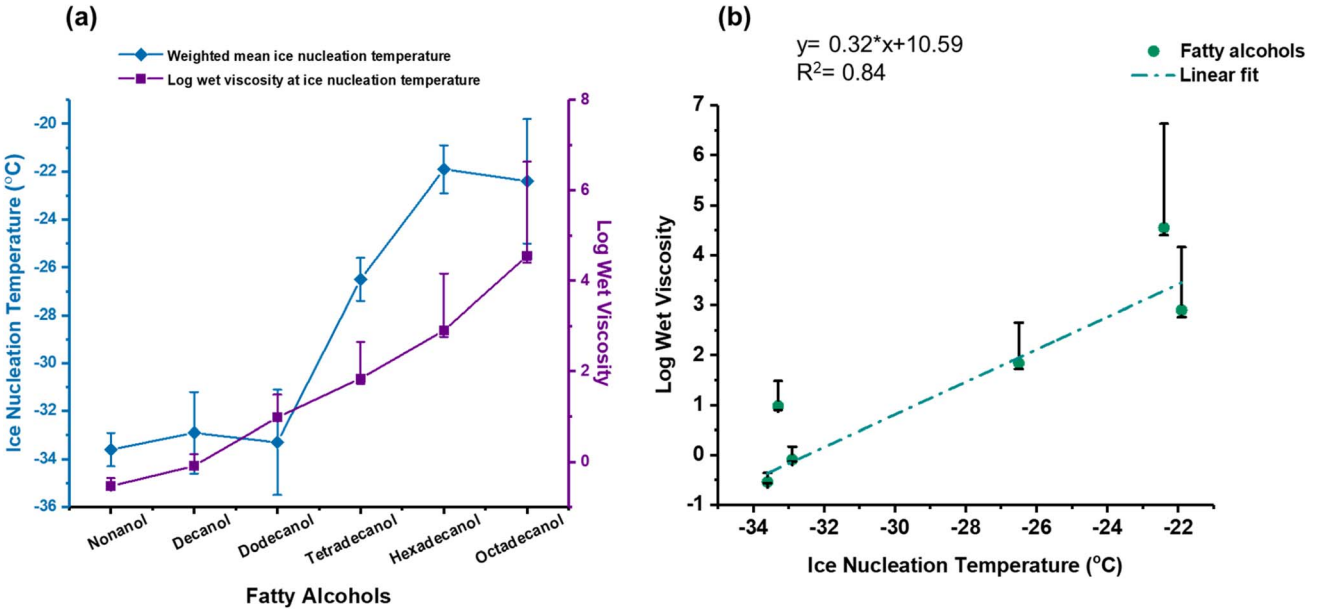

Fig. 6 (a) Depicts ice nucleation temperatures, represented by blue diamonds, and the estimated log wet viscosities at their respective ice nucleation temperatures, depicted by purple squares, and (b) plot of log wet viscosity against ice nucleation temperatures, fitted with a linear regression line, for six fatty alcohols. The uncertainties in the estimated log wet viscosities reflect the uncertainty in the fitting parameters in eqn (1) to calculate the glass transition temperature.[74]

acid, can nucleate ice heterogeneously at low relative humidity, while Wilson *et al.*[95] confirmed that ice nucleation temperature of glassy aerosols is strongly related to their glass transition temperature (T_g), with glass-forming substances such as raffinose and 4-hydroxy-3-methoxy-DL-mandelic acid (HMMA) nucleating ice at temperatures higher than 200 K. Fowler *et al.*[96] and Ignatius *et al.*[62] found that viscous secondary organic aerosols (SOA), such as those from α-pinene, exhibit inhibited ice nucleation at very low temperatures due to restricted particle growth, but can nucleate ice more readily at warmer temperatures. Berkemeier *et al.*[97] concluded that glassy SOA could facilitate heterogeneous ice nucleation up to 225 K, with deposition mode nucleation in glassy states, immersion mode in partially deliquesced states, and homogeneous nucleation in a liquid state. Together, these studies highlight the critical role of aerosol phase and viscosity in determining ice nucleation pathways and efficiency in the atmosphere. Our objective is to explore the relationship between immersion freezing and the phase state of the lipid particles. To elucidate this relationship, we contend that understanding the phase state of the droplet immediately before ice nucleation is essential. Phase state characterization can be achieved through viscosity (η) analysis. Therefore, we employed a theoretical model to determine the wet viscosity (η_{wet}), *i.e.*, the particle's viscosity at equilibrium with the ambient relative humidity at the measured IN temperatures. We generated a plot correlating the ice nucleation temperatures of the fatty alcohols with their respective wet viscosity values to elucidate their relationship, as depicted in Fig. 6(a).

As discussed above, fatty alcohol lipid particles become more effective ice nuclei with increasing chain length. Furthermore, we note a rise in the $\log(\eta_{wet})$ at their corresponding ice nucleation temperatures with increasing chain length. Increased viscosity with molecular size is expected, as viscosity tends to increase due to stronger van der Waals forces between chains of the fatty alcohol, resulting in elevated internal friction. According to the model, log wet viscosity values below 2 indicate a liquid phase state, while values between 2 and 12 suggest a more semi-solid state. The estimated log wet viscosity value for tetradecanol was 1.84, close to the transitional value between liquid and semi-solid phases. Notably, at this point, we observe that fatty alcohol particles begin to exhibit enhanced ice nucleation capabilities. Beyond this transitional point, hexadecanol and octadecanol demonstrate significantly higher wet viscosity values than 2, indicating a semi-solid phase state. Intriguingly, hexadecanol and octadecanol emerge as the most effective ice nuclei (*i.e.*, nucleate ice at warmer temperatures) among the fatty alcohols of interest. These findings align with a prior modeling study that showed more viscous, partially deliquesced, or phase-separated SOA at upper troposphere or lower stratosphere temperatures and relative humidity could nucleate ice more effectively by deposition and immersion freezing.[97] This could be the case here, whereby hydrophobic organic particles with increasing molecular size and viscosity slow relative humidity-induced phase transitions between states as the particles cool by slowing water diffusion into the particles. These organic particles within the droplets form ice crystals heterogeneously at warmer temperatures and lower ice supersaturations than homogeneous freezing. We also attempted to establish a direct correlation between ice nucleation temperatures and wet viscosity by plotting them against each other and fitting them onto a straight line, as depicted in

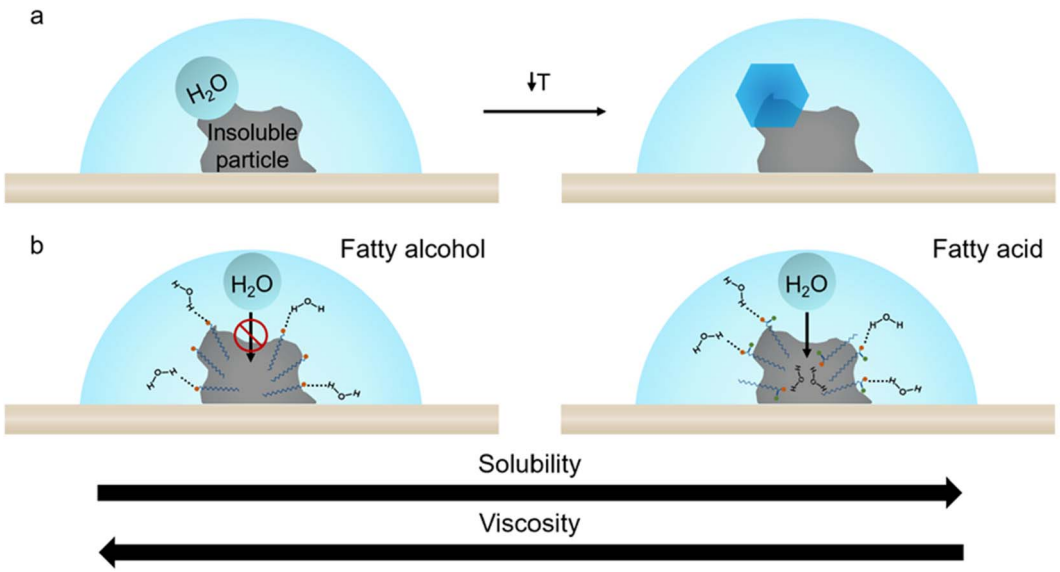

Fig. 7 Conceptual illustration of heterogeneous freezing at a lipid–water interface of insoluble and sparingly soluble particles. (a) An insoluble particle within a water droplet demonstrates ice formation at the lipid–water interface as the temperature decreases. (b) Example of fatty alcohol and fatty acid particles within a water droplet, depicting the orientation of lipids at the interface, where hydrophilic groups (–OH and COOH) of the lipids form hydrogen bonds with water molecules, facilitating ice formation. The fatty acid particle exhibits greater water permeability compared to the fatty alcohol particle due to its higher solubility in water. This increased permeability triggers a positive feedback mechanism, allowing more water to diffuse into the fatty acid particle, which in turn lowers its viscosity. As a result, fatty acid molecules at the interface may reorient their head groups inward, potentially disrupting the lipid particle/water interface and preventing the necessary critical nucleus to form, that would otherwise promote heterogeneous freezing.

Fig. 6(b). The analysis suggests a correlation with a correlation coefficient of 0.84, suggesting, similar to other studies,[93,98] that phase state can play a role in heterogeneous ice nucleation efficacy in immersion freezing.

We found less of a relationship between the much poorer ice nucleating fatty acid particles. Fatty acid ice nucleation temperatures and the estimated logarithm of wet viscosity values by plotting them against each other, as illustrated in Fig. S4(a).† For these poor INPs, the analysis revealed no clear correspondence between ice nucleation and wet viscosity values. Additionally, Fig. S4(b)† provides further evidence of the lack of correlation between ice nucleation and wet viscosity values, with an R-squared value of 0.1. Fatty acid particles are unlikely to exhibit a correlation with viscosity due to their propensity for homogeneous freezing, reaching the homogeneous freezing limit rather than undergoing heterogeneous freezing. This characteristic is significant because viscosity is known to exert a more substantial influence within the temperature range where heterogeneous freezing occurs. Consequently, we anticipate that the impact of viscosity on ice nucleation will be more pronounced for processes involving heterogeneous freezing, which typically occur at temperatures warmer than those associated with homogeneous freezing.

Additionally, Wright and Petters *et al.*[99] previously demonstrated that the ice nucleation temperature for Arizona Test Dust may depend on the cooling rate. Their study showed that increasing the cooling rate from 0.01 K min^{-1} to 5 K min^{-1} resulted in a change in ice nucleation temperature from −24.02 °C to −25.35 °C. However, no error was reported, and there was no apparent difference in the effects of the cooling rate between a different range of 0.05 K min^{-1} and 5 K min^{-1}. Our experiment investigated the immersion ice nucleation of hexadecanol at cooling rates of 3 °C min^{-1} and 10 °C min^{-1}. We found that at these cooling rates, the ice nucleation temperatures overlapped in their standard deviation, −23.3 (±0.7) °C and −21.9 (±1.0) °C, respectively. However, an unpaired *t*-test shows these temperatures were statistically significantly different ($p < 0.0001$). The reason for this difference is unclear, although it can be deduced from previous studies that the cooling rate or time dependence for ice nucleation can affect the number of active ice nucleation sites.[99] This study does not distinguish the effects of cooling rate on the freezing temperatures of the other lipid particles but are compared at a rate of 10 °C min^{-1}.

Conclusions and atmospheric implications

This investigation explored the immersion freezing and IN potential of marine-relevant lipid particles, both fatty alcohols and fatty acids. Previous research has established that monolayers of fatty alcohols exhibit notable IN capabilities, with their effectiveness shown to be chain length dependent.[77,78,81] However, to our knowledge, no studies have been conducted on the freezing behavior of fatty alcohol and fatty acid particles. Our findings reveal a chain length dependence in the IN ability of micron-sized fatty alcohol particles, with longer chains nucleating ice at higher temperatures. However, this

dependence is not as pronounced as previously for monolayers, and the ice nucleating temperatures for the particles are approximately ten degrees lower than that of monolayers.[78,85,100] Compared to fatty alcohol particles, fatty acid particles demonstrate limited efficacy in nucleating ice at warmer temperatures, similar to what has been observed previously. We also utilized frozen fraction curves to gain deeper insights into the characteristics of these ice nuclei. It was noted that certain curves exhibited a tail to higher temperatures. To understand this observation in the frozen fraction curves, we conducted a more detailed analysis of the IN behavior of decanol and octadecanol. Our findings revealed that a higher percentage of smaller droplets nucleate ice at colder temperatures, while larger droplets nucleate ice at warmer temperatures. These results suggest a potential correlation between droplet size and IN temperatures. We also sought to determine the potential influence of the phase state of droplets on their freezing temperatures by estimating their viscosity at their freezing temperature. Our findings revealed a correlation between the phase state of fatty alcohol droplets and IN ability. Our analysis did not reveal any correlation between the phase state and ice nucleation for fatty acids, likely due to their tendency to freeze close to the homogeneous freezing limit. The viscosity effects on ice nucleation are most notable for the fatty alcohol particles, which froze at warmer temperatures than the homogeneous freezing limit compared to the fatty acids and froze at warmer temperatures with increasing predicted viscosity. No such dependence was observed in the fatty acid case. However, this analysis points to a limitation in the viscosity estimation, as it was parameterized from molecular weight, oxygen-to-carbon ratios, and estimated mass-based hygroscopicity parameters. It does not consider the effects of organic anions nor the different functional groups that could modulate viscosity through changes in solubility and water content.[101] In the case of carboxylic acids, which are more soluble than fatty alcohols, it is likely that their viscosities are overestimated.

Solubility also plays an important role in ice nucleation[77,78,81] and may affect the relationships between phase state and ice nucleation of fatty acids and fatty alcohols. Only the fatty alcohols, less soluble than their fatty acid analogs, froze heterogeneously, and their ice nucleation temperatures varied proportionally with chain length and predicted viscosity. The low solubility of fatty acids and fatty alcohols may also influence their effectiveness as ice nuclei.

Recent work by Bieber *et al.*[102] suggests that the ice nucleation mechanism of the bacterium *Pseudomonas syringae* is likely induced by larger aggregates and fragments within the droplet volume. Their findings also indicate that Snomax, a protein derived from the bacterium, aligns at the air–water interface and nucleates ice there. Using hyperspectral imaging, their study successfully pinpointed the origin of the ice nucleation site. Although our study does not pinpoint the exact origin of ice nucleation, the data suggests a conceptual understanding of the process. The migration of components to the air–water interface, water uptake, and the freezing process depend on the particle's solubility, droplet surface tension, and the phase of the particle immersed in the droplet at the freezing temperature.

In Perkins *et al.*,[85] fatty acids mixed with fatty alcohols applied as a monolayer to liquid water droplets depressed the freezing temperature of the fatty alcohols. It was suggested that the fatty alcohols form monolayers resembling the hexagonal ice crystal structure, which leads to warmer freezing temperatures. Both fatty alcohols and acids in this study exhibit surface activity. This increased surface activity, compared to that of liquid water, could impact the water uptake properties of the nucleus, a process influenced by temperature.[103] Carboxylic acids, more polar than their alcohol counterparts, form more hydrogen bonds with water molecules and dissolve more readily in water.

We hypothesize, supported by our data, that the insoluble fatty alcohols freeze at warmer temperatures than the fatty acids, partly by inducing heterogeneous nucleation at the lipid particle–water interface within the droplet, as opposed to the air–water interface of fatty alcohol monolayers studied in Perkins *et al.*,[85] or within the droplet volume of more soluble fatty acid particles. A conceptual depiction of this process is shown in Fig. 7. The predicted elevated viscosities of the semi-solids (*i.e.*, $\log(\eta) \geq 2.0$), particularly the insoluble fatty alcohols, suggest limited diffusion of water into the particles. Due to their low solubility and high viscosity, liquid water accumulates along the fatty alcohol particle interface, with hydrophilic –OH groups oriented toward this interface and the hydrophobic tails remaining within the particle. This orientation may favor heterogeneous ice formation by aligning with the basal plane of ice. In contrast, more acidic analogues, while exhibiting similar predicted viscosity, are more water-soluble. Water diffuses more readily into the fatty acid particles, where the molecules dissociate and dissolve more easily, potentially raising the barrier for ice nucleation and resulting in lower activation temperatures.

Research indicates that organic aerosol emissions from oceans suggest marine INPs could play a significant role in facilitating ice-phase transitions in clouds, particularly in oceanic regions devoid of terrestrial aerosol sources, such as the Southern Ocean.[3,4,17,18,26] In natural environments, fatty acids and fatty alcohols are integral components of biological membranes and organic matter.[52,54–57] Their presence in atmospheric aerosols and on surfaces can significantly impact cloud formation and precipitation processes, thus playing a crucial role in climate and weather studies.[3,4,15] The hydrocarbon chains in fatty acids and fatty alcohols can organize into structures resembling ice's crystalline structure.[83] This structural similarity reduces the energy barrier for ice nucleation, facilitating the formation of ice crystals.

This study investigates the influence of chain length and the viscosity of lipid particles on INPs naturally present in nascent SSA. Limited research had been done previously to understand the impact of phase state on heterogeneous ice nucleation.[58–60,62] We utilized a theoretical model to calculate the wet viscosity of lipid particles and examined their effect on immersion ice nucleation. This study indicates that the more viscous phase states of organic aerosol components that freeze at temperatures warmer than the homogeneous freezing limit

are potentially better ice nuclei, providing a foundation for further investigation into the significant impact of phase state on this process. We have previously demonstrated that the organic matter in SSA can vary in viscosity depending on the amount of algal biomass in the seawater, becoming more viscous with increasing biomass and increasing molecular weight of organic matter within the particles.[104] It follows from this study that a potentially larger fraction of SSA would be expected to nucleate ice heterogeneously during phytoplankton blooms. This was shown in a previous study, demonstrating higher INP fractions from SSA during the peak of a phytoplankton bloom in a marine aerosol reference tank.[18] Another study independently concluded that the SSA components from phytoplankton blooms in the North Atlantic Ocean during late spring facilitate IN activity.[105] Future research should explore the immersion ice nucleation behavior of atmospherically relevant particles while concurrently determining their phase state to more accurately assess the impact of phase state on immersion ice nucleation.

Data availability

Data for this article, including microscopy images and tabulated freezing temperatures, and data used in the figures are available at OSF at **https://osf.io/pqn7v/**.

Author contributions

L. M., J. H. S. and V. G. designed experiments and L. M., A. L. carried out the experiments. The manuscript was written through the contributions of all authors. All authors have given approval to the final version of the manuscript.

Conflicts of interest

There are no conflicts to declare.

Acknowledgements

This research received support from the National Science Foundation (NSF) through the NSF Center for Aerosol Impacts on the Chemistry of the Environment (NSF-CAICE), designated as a Center for Chemical Innovation (CHE-1801971). The authors extend their gratitude to CAICE collaborators, notably Dr Paul DeMott. The views and opinions expressed in this material solely belong to the authors and do not necessarily represent the opinions, findings, or conclusions of the National Science Foundation.

References

1 U. Lohmann and J. Feichter, Global Indirect Aerosol Effects: A Review, *Atmos. Chem. Phys.*, 2005, 5(3), 715–737, DOI: **10.5194/ACP-5-715-2005**.

2 P. J. DeMott, R. H. Mason, C. S. McCluskey, T. C. J. Hill, R. J. Perkins, Y. Desyaterik, A. K. Bertram, J. V. Trueblood, V. H. Grassian, Y. Qiu, V. Molinero, Y. Tobo, C. M. Sultana, C. Lee and K. A. Prather, Ice Nucleation by Particles Containing Long-Chain Fatty Acids of Relevance to Freezing by Sea Spray Aerosols, *Environ. Sci.: Processes Impacts*, 2018, **20**(11), 1559–1569, DOI: **10.1039/C8EM00386F**.

3 T. W. Wilson, L. A. Ladino, P. A. Alpert, M. N. Breckels, I. M. Brooks, J. Browse, S. M. Burrows, K. S. Carslaw, J. A. Huffman, C. Judd, W. P. Kilthau, R. H. Mason, G. McFiggans, L. A. Miller, J. J. Nájera, E. Polishchuk, S. Rae, C. L. Schiller, M. Si, J. V. Temprado, T. F. Whale, J. P. S. Wong, O. Wurl, J. D. Yakobi-Hancock, J. P. D. Abbatt, J. Y. Aller, A. K. Bertram, D. A. Knopf and B. J. Murray, A Marine Biogenic Source of Atmospheric Ice-Nucleating Particles, *Nature*, 2015, **525**(7568), 234–238, DOI: **10.1038/nature14986**.

4 S. M. Burrows, C. Hoose, U. Pöschl and M. G. Lawrence, Ice Nuclei in Marine Air: Biogenic Particles or Dust?, *Atmos. Chem. Phys.*, 2013, **13**(1), 245–267, DOI: **10.5194/ACP-13-245-2013**.

5 D. O'Sullivan, B. J. Murray, T. L. Malkin, T. F. Whale, N. S. Umo, J. D. Atkinson, H. C. Price, K. J. Baustian, J. Browse and M. E. Webb, Ice Nucleation by Fertile Soil Dusts: Relative Importance of Mineral and Biogenic Components, *Atmos. Chem. Phys.*, 2014, **14**(4), 1853–1867, DOI: **10.5194/acp-14-1853-2014**.

6 P. J. DeMott, A. J. Prenni, X. Liu, S. M. Kreidenweis, M. D. Petters, C. H. Twohy, M. S. Richardson, T. Eidhammer and D. C. Rogers, Predicting Global Atmospheric Ice Nuclei Distributions and Their Impacts on Climate, *Proc. Natl. Acad. Sci. U. S. A.*, 2010, **107**(25), 11217–11222, DOI: **10.1073/PNAS.0910818107/-/DCSUPPLEMENTAL/PNAS.0910818107_SI.PDF**.

7 X. Wang, C. M. Sultana, J. Trueblood, T. C. J. Hill, F. Malfatti, C. Lee, O. Laskina, K. A. Moore, C. M. Beall, C. S. McCluskey, G. C. Cornwell, Y. Zhou, J. L. Cox, M. A. Pendergraft, M. V. Santander, T. H. Bertram, C. D. Cappa, F. Azam, P. J. DeMott, V. H. Grassian and K. A. Prather, Microbial Control of Sea Spray Aerosol Composition: A Tale of Two Blooms, *ACS Cent. Sci.*, 2015, **1**(3), 124–131, DOI: **10.1021/acscentsci.5b00148**.

8 P. J. DeMott, D. J. Cziczo, A. J. Prenni, D. M. Murphy, S. M. Kreidenweis, D. S. Thomson, R. Borys and D. C. Rogers, Measurements of the Concentration and Composition of Nuclei for Cirrus Formation, *Proc. Natl. Acad. Sci. U. S. A.*, 2003, **100**(25), 14655–14660, DOI: **10.1073/PNAS.2532677100/ASSET/C338FF43-111A-404F-924A-5C2431501537/ASSETS/GRAPHIC/PQ2532677006.JPEG**.

9 B. J. Murray, D. O'sullivan, J. D. Atkinson and M. E. Webb, Ice Nucleation by Particles Immersed in Supercooled Cloud Droplets, *Chem. Soc. Rev.*, 2012, **41**(19), 6519–6554, DOI: **10.1039/C2CS35200A**.

10 O. Boucher, D. Randall, P. Artaxo, C. Bretherton, G. Feingold, P. Forster, V.-M. Kerminen, Y. Kondo, H. Liao, U. Lohmann, P. Rasch, S. K. Satheesh, S. Sherwood, B. Stevens, X. Y. Zhang, T. F. Stocker, D. Qin, G.-K. Plattner, M. Tignor, S. Allen and

J. Boschung, Clouds and Aerosols, in, *Climate Change 2013, The Physical Science Basis, Contribution of Working Group I to the Fifth Assessment Report of the Intergovernmental Panel on Climate Change*, 2013, **https://www.ipcc.ch/site/assets/uploads/2018/02/WG1AR5_Chapter07_FINAL-1.pdf**.

11 B. G. Pummer, C. Budke, S. Augustin-Bauditz, D. Niedermeier, L. Felgitsch, C. J. Kampf, R. G. Huber, K. R. Liedl, T. Loerting, T. Moschen, M. Schauperl, M. Tollinger, C. E. Morris, H. Wex, H. Grothe, U. Pöschl, T. Koop and J. Fröhlich-Nowoisky, Ice Nucleation by Water-Soluble Macromolecules, *Atmos. Chem. Phys.*, 2015, **15**(8), 4077–4091, DOI: **10.5194/acp-15-4077-2015**.

12 B. A. Mitts, X. Wang, D. D. Lucero, C. M. Beall, G. B. Deane, P. J. DeMott and K. A. Prather, Importance of Supermicron Ice Nucleating Particles in Nascent Sea Spray, *Geophys. Res. Lett.*, 2021, **48**(3), 1–10, DOI: **10.1029/2020GL089633**.

13 D. A. Knopf, P. A. Alpert, B. Wang and J. Y. Aller, Stimulation of Ice Nucleation by Marine Diatoms, *Nat. Geosci.*, 2011, **4**(2), 88–90, DOI: **10.1038/ngeo1037**.

14 D. B. Collins, D. F. Zhao, M. J. Ruppel, O. Laskina, J. R. Grandquist, R. L. Modini, M. D. Stokes, L. M. Russell, T. H. Bertram, V. H. Grassian, G. B. Deane and K. A. Prather, Direct Aerosol Chemical Composition Measurements to Evaluate the Physicochemical Differences between Controlled Sea Spray Aerosol Generation Schemes, *Atmos. Meas. Tech.*, 2014, **7**(11), 3667–3683, DOI: **10.5194/amt-7-3667-2014**.

15 D. A. Knopf, P. A. Alpert and B. Wang, The Role of Organic Aerosol in Atmospheric Ice Nucleation: A Review, *ACS Earth Space Chem.*, 2018, **2**(3), 168–202, DOI: **10.1021/ACSEARTHSPACECHEM.7B00120**.

16 D. A. Knopf and P. A. Alpert, Atmospheric Ice Nucleation, *Nat. Rev. Phys.*, 2023, **5**(4), 203–217, DOI: **10.1038/s42254-023-00570-7**.

17 C. S. McCluskey, T. C. J. Hill, F. Malfatti, C. M. Sultana, C. Lee, M. V. Santander, C. M. Beall, K. A. Moore, G. C. Cornwell, D. B. Collins, K. A. Prather, T. Jayarathne, E. A. Stone, F. Azam, S. M. Kreidenweis and P. J. DeMott, A Dynamic Link between Ice Nucleating Particles Released in Nascent Sea Spray Aerosol and Oceanic Biological Activity during Two Mesocosm Experiments, *J. Atmos. Sci.*, 2017, **74**(1), 151–166, DOI: **10.1175/JAS-D-16-0087.1**.

18 P. J. DeMott, T. C. J. Hill, C. S. McCluskey, K. A. Prather, D. B. Collins, R. C. Sullivan, M. J. Ruppel, R. H. Mason, V. E. Irish, T. Lee, C. Y. Hwang, T. S. Rhee, J. R. Snider, G. R. McMeeking, S. Dhaniyala, E. R. Lewis, J. J. B. Wentzell, J. Abbatt, C. Lee, C. M. Sultana, A. P. Ault, J. L. Axson, M. D. Martinez, I. Venero, G. Santos-Figueroa, M. D. Stokes, G. B. Deane, O. L. Mayol-Bracero, V. H. Grassian, T. H. Bertram, A. K. Bertram, B. F. Moffett and G. D. Franc, Sea Spray Aerosol as a Unique Source of Ice Nucleating Particles, *Proc. Natl. Acad. Sci. U. S. A.*, 2016, **113**(21), 5797–5803, DOI: **10.1073/PNAS.1514034112/-/DCSUPPLEMENTAL**.

19 G. Vali, P. J. DeMott, O. Möhler and T. F. Whale, Technical Note: A Proposal for Ice Nucleation Terminology, *Atmos. Chem. Phys.*, 2015, **15**(18), 10263–10270, DOI: **10.5194/acp-15-10263-2015**.

20 J. Gilmour, *Microphysics of Clouds and Precipitation*, 1980, vol. 31, DOI: **10.1088/0031-9112/31/5/037**.

21 N. Hiranuma, O. Möhler, H. Bingemer, U. Bundke, D. J. Cziczo, A. Danielczok, M. Ebert, S. Garimella, N. Hoffmann, K. Höhler, Z. A. Kanji, A. Kiselev, M. Raddatz and O. Stetzer, Immersion Freezing of Clay Minerals and Bacterial Ice Nuclei, *AIP Conf. Proc.*, 2013, **1527**, 914–917, DOI: **10.1063/1.4803420**.

22 Z. A. Kanji, L. A. Ladino, H. Wex, Y. Boose, M. Burkert-Kohn, D. J. Cziczo and M. Krämer, Overview of Ice Nucleating Particles, *Meteorol. Monogr.*, 2017, **58**, 1(1)–1(33), DOI: **10.1175/amsmonographs-d-16-0006.1**.

23 A. Ansmann, M. Tesche, D. Althausen, D. Müller, P. Seifert, V. Freudenthaler, B. Heese, M. Wiegner, G. Pisani, P. Knippertz and O. Dubovik, Influence of Saharan Dust on Cloud Glaciation in Southern Morocco during the Saharan Mineral Dust Experiment, *J. Geophys. Res.: Atmos.*, 2008, **113**(4), 1–16, DOI: **10.1029/2007JD008785**.

24 H. Morrison, G. De Boer, G. Feingold, J. Harrington, M. D. Shupe and K. Sulia, Resilience of Persistent Arctic Mixed-Phase Clouds, *Nat. Geosci.*, 2012, **5**(1), 11–17, DOI: **10.1038/ngeo1332**.

25 C. D. Westbrook and A. J. Illingworth, The Formation of Ice in a Long-Lived Supercooled Layer Cloud, *Q. J. R. Meteorol. Soc.*, 2013, **139**(677), 2209–2221, DOI: **10.1002/qj.2096**.

26 C. S. McCluskey, J. Ovadnevaite, M. Rinaldi, J. Atkinson, F. Belosi, D. Ceburnis, S. Marullo, T. C. J. Hill, U. Lohmann, Z. A. Kanji, C. O'Dowd, S. M. Kreidenweis and P. J. DeMott, Marine and Terrestrial Organic Ice-Nucleating Particles in Pristine Marine to Continentally Influenced Northeast Atlantic Air Masses, *J. Geophys. Res.: Atmos.*, 2018, **123**(11), 6196–6212, DOI: **10.1029/2017JD028033**.

27 V. E. Irish, S. J. Hanna, Y. Xi, M. Boyer, E. Polishchuk, M. Ahmed, J. Chen, J. P. D. Abbatt, M. Gosselin, R. Chang, L. A. Miller and A. K. Bertram, Revisiting Properties and Concentrations of Ice-Nucleating Particles in the Sea Surface Microlayer and Bulk Seawater in the Canadian Arctic during Summer, *Atmos. Chem. Phys.*, 2019, **19**(11), 7775–7787, DOI: **10.5194/ACP-19-7775-2019**.

28 J. Vergara-Temprado, B. J. Murray, T. W. Wilson, D. O'Sullivan, J. Browse, K. J. Pringle, K. Ardon-Dryer, A. K. Bertram, S. M. Burrows, D. Ceburnis, P. J. Demott, R. H. Mason, C. D. O'Dowd, M. Rinaldi and K. S. Carslaw, Contribution of Feldspar and Marine Organic Aerosols to Global Ice Nucleating Particle Concentrations, *Atmos. Chem. Phys.*, 2017, **17**(5), 3637–3658, DOI: **10.5194/acp-17-3637-2017**.

29 A. H. Callaghan, M. D. Stokes and G. B. Deane, The Effect of Water Temperature on Air Entrainment, Bubble Plumes, and Surface Foam in a Laboratory Breaking-Wave Analog, *J. Geophys. Res.*, 2014, **119**(11), 7463–7482, DOI: **10.1002/2014jc010351**.

30 K. A. Prather, T. H. Bertram, V. H. Grassian, G. B. Deane, M. D. Stokes, P. J. DeMott, L. I. Aluwihare, B. P. Palenik,

F. Azam, J. H. Seinfeld, R. C. Moffet, M. J. Molina, C. D. Cappa, F. M. Geiger, G. C. Roberts, L. M. Russell, A. P. Ault, J. Baltrusaitis, D. B. Collins, C. E. Corrigan, L. A. Cuadra-Rodriguez, C. J. Ebben, S. D. Forestieri, T. L. Guasco, S. P. Hersey, M. J. Kim, W. F. Lambert, R. L. Modini, W. Mui, B. E. Pedler, M. J. Ruppel, O. S. Ryder, N. G. Schoepp, R. C. Sullivan and D. Zhao, Bringing the Ocean into the Laboratory to Probe the Chemical Complexity of Sea Spray Aerosol, *Proc. Natl. Acad. Sci. U. S. A.*, 2013, **110**(19), 7550–7555, DOI: **10.1073/PNAS.1300262110/-/DCSUPPLEMENTAL**.

31 P. K. Quinn, D. B. Collins, V. H. Grassian, K. A. Prather and T. S. Bates, Chemistry and Related Properties of Freshly Emitted Sea Spray Aerosol, *Chem. Rev.*, 2015, **115**(10), 4383–4399, DOI: **10.1021/CR500713G**.

32 B. Gantt and N. Meskhidze, The Physical and Chemical Characteristics of Marine Primary Organic Aerosol : A Review, *Atmos. Chem. Phys.*, 2013, **13**(8), 3979–3996, DOI: **10.5194/acp-13-3979-2013**.

33 G. de Leeuw, E. L. Andreas, M. D. Anguelova, C. W. Fairall, E. R. Lewis, C. O'Dowd, M. Schulz and S. E. Schwartz, Production Flux of Sea Spray Aerosol, *Rev. Geophys.*, 2011, **49**(2), 1–39, DOI: **10.1029/2010RG000349**.

34 P. A. Alpert, J. Y. Aller and D. A. Knopf, Ice Nucleation from Aqueous NaCl Droplets with and without Marine Diatoms, *Atmos. Chem. Phys.*, 2011, **11**(12), 5539–5555, DOI: **10.5194/acp-11-5539-2011**.

35 D. A. Knopf, P. A. Alpert, B. Wang, R. E. O. Brien, S. T. Kelly, A. Laskin, M. K. Gilles and R. C. Moffet, Microspectroscopic Imaging and Characterization of Individually Identified Ice Nucleating Particles from a Case Field Study, *J. Geophys. Res.: Atmos.*, 2014, **119**(17), 365–381, DOI: **10.1002/2014jd021866**.

36 L. A. Ladino, J. D. Yakobi-hancock, W. P. Kilthau, R. H. Mason, M. Si, J. Li, L. A. Miller, C. L. Schiller, J. A. Huffman, J. Y. Aller, D. A. Knopf, A. K. Bertram and J. P. D. Abbatt, Addressing the Ice Nucleating Abilities of Marine Aerosol : A Combination of Deposition Mode Laboratory and Field Measurements, *Atmos. Environ.*, 2016, **132**, 1–10, DOI: **10.1016/j.atmosenv.2016.02.028**.

37 C. S. McCluskey, E. T. C. J. Hill, C. M. Sultana, O. Laskina, J. Trueblood, M. V. Santander, C. M. Beall, J. M. Michaud, S. M. Kreidenweis, K. A. Prather, V. Grassian and P. J. Demott, A Mesocosm Double Feature: Insights into the Chemical Makeup of Marine Ice Nucleating Particles, *J. Atmos. Sci.*, 2018, **75**(7), 2405–2423, DOI: **10.1175/JAS-D-17-0155.1**.

38 P. Roy, L. E. Mael, T. C. J. Hill, L. Mehndiratta, G. Peiker, M. L. House, P. J. DeMott, V. H. Grassian and C. S. Dutcher, Ice Nucleating Activity and Residual Particle Morphology of Bulk Seawater and Sea Surface Microlayer, *ACS Earth Space Chem.*, 2021, **5**(8), 1916–1928, DOI: **10.1021/acsearthspacechem.1c00175**.

39 J. V. Trueblood, A. Nicosia, A. Engel, B. Zäncker, M. Rinaldi, E. Freney, M. Thyssen, I. Obernosterer, J. Dinasquet, F. Belosi, A. Tovar-Sánchez, A. Rodriguez-Romero, G. Santachiara, C. Guieu and K. Sellegri, A Two-Component Parameterization of Marine Ice-Nucleating Particles Based on Seawater Biology and Sea Spray Aerosol Measurements in the Mediterranean Sea, *Atmos. Chem. Phys.*, 2021, **21**(6), 4659–4676, DOI: **10.5194/acp-21-4659-2021**.

40 M. C. Facchini, M. Rinaldi, S. Decesari, C. Carbone, E. Finessi, M. Mircea, S. Fuzzi, D. Ceburnis, R. Flanagan, E. D. Nilsson, G. D. Leeuw, M. Martino, J. Woeltjen and C. D. O. Dowd, Primary Submicron Marine Aerosol Dominated by Insoluble Organic Colloids and Aggregates, *Geophys. Res. Lett.*, 2008, **35**(17), 1–5, DOI: **10.1029/2008GL034210**.

41 S. Decesari, M. Rinaldi, C. Carbone, S. Fuzzi, F. Moretti, E. Tagliavini, D. Ceburnis and C. D. O. Dowd, Important Source of Marine Secondary Organic Aerosol from Biogenic Amines, *Environ. Sci. Technol.*, 2008, **42**(24), 9116–9121, DOI: **10.1021/es8018385**.

42 M. Mochida, Y. Kitamori and K. Kawamura, Fatty Acids in the Marine Atmosphere : Factors Governing Their Concentrations and Evaluation of Organic Films on Sea-Salt Particles, *J. Geophys. Res.*, 2002, **107**(D17), 1–10, DOI: **10.1029/2001JD001278**.

43 B. Gantt and N. Meskhidze, Atmospheric Chemistry and Physics Climate of the Past Geoscientific Instrumentation Methods and Data Systems The Physical and Chemical Characteristics of Marine Primary Organic Aerosol: A Review, *Atmos. Chem. Phys.*, 2013, **13**(8), 3979–3996, DOI: **10.5194/acp-13-3979-2013**.

44 A. P. Ault, R. C. Moffet, J. Baltrusaitis, D. B. Collins, M. J. Ruppel, L. A. Cuadra-Rodriguez, D. Zhao, T. L. Guasco, C. J. Ebben, F. M. Geiger, T. H. Bertram, K. A. Prather and V. H. Grassian, Size-Dependent Changes in Sea Spray Aerosol Composition and Properties with Different Seawater Conditions, *Environ. Sci. Technol.*, 2013, **47**(11), 5603–5612, DOI: **10.1021/ES400416G/SUPPL_FILE/ES400416G_SI_001.PDF**.

45 F. Cavalli, M. C. Facchini, S. Decesari, M. Mircea, L. Emblico and S. Fuzzi, Advances in Characterization of Size-Resolved Organic Matter in Marine Aerosol over the North Atlantic, *J. Geophys. Res.*, 2004, **109**(D24), 1–14, DOI: **10.1029/2004JD005137**.

46 L. M. Russell, R. Bahadur and P. J. Ziemann, Identifying Organic Aerosol Sources by Comparing Functional Group Composition in Chamber and Atmospheric Particles, *Proc. Natl. Acad. Sci. U. S. A.*, 2011, **108**(9), 3516–3521, DOI: **10.1073/pnas.1006461108**.

47 L. N. Hawkins and L. M. Russell, Polysaccharides , Proteins , and Phytoplankton Fragments : Four Chemically Distinct Types of Marine Primary Organic Aerosol Classified by Single Particle Spectromicroscopy, *Adv. Meteorol.*, 2010, **2010**, 1–14, DOI: **10.1155/2010/612132**.

48 M. D. Stokes, G. B. Deane, K. Prather, T. H. Bertram, M. J. Ruppel, O. S. Ryder, J. M. Brady and D. A. Zhao, Marine Aerosol Reference Tank System as a Breaking Wave Analogue for the Production of Foam and Sea-Spray Aerosols Climate, *Atmos. Meas. Tech.*, 2013, **6**(4), 1085–1094, DOI: **10.5194/amt-6-1085-2013**.

49 T. Jayarathne, C. M. Sultana, C. Lee, F. Malfatti, J. L. Cox, M. A. Pendergraft, K. A. Moore, F. Azam, A. V. Tivanski, C. D. Cappa, T. H. Bertram, V. H. Grassian, K. A. Prather and E. A. Stone, Enrichment of Saccharides and Divalent Cations in Sea Spray Aerosol during Two Phytoplankton Blooms, *Environ. Sci. Technol.*, 2016, **50**(21), 11511–11520, DOI: **10.1021/acs.est.6b02988**.

50 R. E. Cochran, O. Laskina, T. Jayarathne, A. Laskin, J. Laskin, P. Lin, C. Sultana, C. Lee, K. A. Moore, C. D. Cappa, T. H. Bertram, K. A. Prather, V. H. Grassian and E. A. Stone, Analysis of Organic Anionic Surfactants in Fine and Coarse Fractions of Freshly Emitted Sea Spray Aerosol, *Environ. Sci. Technol.*, 2016, **50**(5), 2477–2486, DOI: **10.1021/acs.est.5b04053**.

51 L. M. Russell, L. N. Hawkins, A. A. Frossard, P. K. Quinn and T. S. Bates, Carbohydrate-like Composition of Submicron Atmospheric Particles and Their Production from Ocean Bubble Bursting, *Proc. Natl. Acad. Sci. U. S. A.*, 2010, **107**(15), 6652–6657, DOI: **10.1073/pnas.0908905107**.

52 R. E. Cochran, O. Laskina, J. V. Trueblood, A. D. Estillore, H. S. Morris, T. Jayarathne, C. M. Sultana, C. Lee, P. Lin, J. Laskin, A. Laskin, J. A. Dowling, Z. Qin, C. D. Cappa, T. H. Bertram, A. V. Tivanski, E. A. Stone, K. A. Prather and V. H. Grassian, Molecular Diversity of Sea Spray Aerosol Particles: Impact of Ocean Biology on Particle Composition and Hygroscopicity, *Chem*, 2017, **2**(5), 655–667, DOI: **10.1016/j.chempr.2017.03.007**.

53 P. K. Quinn, T. S. Bates, K. S. Schulz, D. J. Co, A. A. Frossard, L. M. Russell, W. C. Keene and D. J. Kieber, Contribution of Sea Surface Carbon Pool to Organic Matter Enrichment in Sea Spray Aerosol, *Nat. Geosci.*, 2014, **7**(3), 228–232, DOI: **10.1038/NGEO2092**.

54 W. D. Garrett, The Organic Chemical Composition of the Ocean Surface, *Deep-Sea Res. Oceanogr. Abstr.*, 1967, **14**(2), 221–227, DOI: **10.1016/0011-7471(67)90007-1**.

55 N. L. Jar, W. D. Garrett, M. A. Scheiman and C. Timmons, SURFACE CHEMICAL CHARACTERIZATION of SURFACE-ACTIVE MATERIAL in SEAWATER, *Limnol. Oceanogr.*, 1967, **12**(1), 88–96, DOI: **10.4319/lo.1967.12.1.0088**.

56 R. B. Gagosian, O. C. Zafiriou, E. T. Peltzer and J. B. Alford, Lipids in Aerosols from the Tropical North Pacific: Temporal Variability, *J. Geophys. Res.*, 1982, **87**(C13), 11133, DOI: **10.1029/jc087ic13p11133**.

57 R. B. Gagosian, Particle Size Distribution of Lipids in Aerosols off the Coast of Peru, *J. Geophys. Res.: Atmos.*, 1985, **90**(D5), 7889–7898, DOI: **10.1029/jd090id05p07889**.

58 J. P. Reid, A. K. Bertram, D. O. Topping, A. Laskin, S. T. Martin, M. D. Petters, F. D. Pope and G. Rovelli, The Viscosity of Atmospherically Relevant Organic Particles, *Nat. Commun.*, 2018, **9**(1), 1–14, DOI: **10.1038/s41467-018-03027-z**.

59 D. M. Lienhard, A. J. Huisman, U. K. Krieger, Y. Rudich, C. Marcolli, B. P. Luo, D. L. Bones, J. P. Reid, A. T. Lambe, M. R. Canagaratna, P. Davidovits, T. B. Onasch, D. R. Worsnop, S. S. Steimer, T. Koop and T. Peter, Viscous Organic Aerosol Particles in the Upper Troposphere: Diffusivity-Controlled Water Uptake and Ice Nucleation?, *Atmos. Chem. Phys.*, 2015, **15**(23), 13599–13613, DOI: **10.5194/acp-15-13599-2015**.

60 R. Wagner, O. Möhler, H. Saathoff, M. Schnaiter, J. Skrotzki, T. Leisner, T. W. Wilson, T. L. Malkin and B. J. Murray, Ice Cloud Processing of Ultra-Viscous/Glassy Aerosol Particles Leads to Enhanced Ice Nucleation Ability, *Atmos. Chem. Phys.*, 2012, **12**(18), 8589–8610, DOI: **10.5194/acp-12-8589-2012**.

61 T. Koop, B. Luo, A. Tsias and T. Peter, Water Activity as the Determinant for Homogeneous Ice Nucleation in Aqueous Solutions, *Nature*, 2000, **406**(6796), 611–614, DOI: **10.1038/35020537**.

62 K. Ignatius, T. B. Kristensen, E. Järvinen, L. Nichman, C. Fuchs, H. Gordon, P. Herenz, C. R. Hoyle, J. Duplissy, S. Garimella, A. Dias, C. Frege, N. Höppel, J. Tröstl, R. Wagner, C. Yan, A. Amorim, U. Baltensperger, J. Curtius, N. M. Donahue, M. W. Gallagher, J. Kirkby, M. Kulmala, O. Möhler, H. Saathoff, M. Schnaiter, A. Tomé, A. Virtanen, D. Worsnop and F. Stratmann, Heterogeneous Ice Nucleation of Viscous Secondary Organic Aerosol Produced from Ozonolysis of α-Pinene, *Atmos. Chem. Phys.*, 2016, **16**(10), 6495–6509, DOI: **10.5194/acp-16-6495-2016**.

63 K. J. Baustian, M. E. Wise and M. A. Tolbert, Depositional Ice Nucleation on Solid Ammonium Sulfate and Glutaric Acid Particles, *Atmos. Chem. Phys.*, 2010, **10**(5), 2307–2317, DOI: **10.5194/acp-10-2307-2010**.

64 L. E. Mael, H. Busse and V. H. Grassian, Measurements of Immersion Freezing and Heterogeneous Chemistry of Atmospherically Relevant Single Particles with Micro-Raman Spectroscopy, *Anal. Chem.*, 2019, **91**(17), 11138–11145, DOI: **10.1021/acs.analchem.9b01819**.

65 L. E. Mael, G. Peiker, H. L. Busse and V. H. Grassian, Temperature-Dependent Liquid Water Structure for Individual Micron-Sized, Supercooled Aqueous Droplets with Inclusions, *J. Phys. Chem. A*, 2021, **125**, 31, DOI: **10.1021/acs.jpca.1c08331**.

66 L. E. Mael, H. L. Busse, G. Peiker and V. H. Grassian, Low-Temperature Water Uptake of Individual Marine and Biologically Relevant Atmospheric Particles Using Micro-Raman Spectroscopy, *J. Phys. Chem. A*, 2021, **125**(44), 9691–9699, DOI: **10.1021/acs.jpca.1c08037**.

67 L. E. Mael, *Micro-Raman Spectroscopy as a Probe of the Composition, Ice Nucleation, and Low Temperature Water Uptake of Individual Substrate Deposited Aerosol Particles*, Univ. Calif. San Diego, 2021.

68 S. T. Martin, Phase Transitions of Aqueous Atmospheric Particles, *Chem. Rev.*, 2000, **100**(9), 3403–3454, DOI: **10.1021/cr990034t**.

69 P. K. Narayanaswamy, The Raman Spectra of Water, Heavy Water and Ice, *Proc. Indian Acad. Sci.*, 1948, **27**(4), 311–315, DOI: **10.1007/bf03171021**.

70 B. Minčeva-Šukarova, W. F. Sherman and G. R. Wilkinson, The Raman Spectra of Ice (Ih, II, III, V, VI and IX) as Functions of Pressure and Temperature, *J. Phys. C: Solid State Phys.*, 1984, **17**(32), 5833–5850, DOI: **10.1088/0022-3719/17/32/017**.

71 N. Ockman, The Infra-Red and Raman Spectra of Ice, *Adv. Phys.*, 2006, **7**(26), 199–220, DOI: **10.1080/00018735800101227**.
72 B. Zobrist, C. Marcolli, D. A. Pedernera and T. Koop, Do Atmospheric Aerosols Form Glasses ?, *Atmos. Chem. Phys.*, 2008, **8**(17), 5221–5244, DOI: **10.5194/acp-8-5221-2008**.
73 T. Koop, J. Bookhold, M. Shiraiwa and U. P. Pöschl, Glass Transition and Phase State of Organic Compounds: Dependency on Molecular Properties and Implications for Secondary Organic Aerosols in the Atmosphere, *Phys. Chem. Chem. Phys.*, 2011, **13**(43), 19238, DOI: **10.1039/c1cp22617g**.
74 M. Shiraiwa, Y. Li, A. P. Tsimpidi, V. A. Karydis, T. Berkemeier, S. N. Pandis, J. Lelieveld, T. Koop and U. Po, Global Distribution of Particle Phase State in Atmospheric Secondary Organic Aerosols, *Nat. Commun.*, 2017, **8**(1), 1–7, DOI: **10.1038/ncomms15002**.
75 W. W. Derieux, Y. Li, P. Lin, J. Laskin, A. Laskin and A. K. Bertram, Predicting the Glass Transition Temperature and Viscosity of Secondary Organic Material Using Molecular Composition, *Atmos. Chem. Phys.*, 2018, **18**(9), 6331–6351, DOI: **10.5194/acp-18-6331-2018**.
76 E. Mikhailov, S. Vlasenko and D. Rose, Mass-Based Hygroscopicity Parameter Interaction Model and Measurement of Atmospheric Aerosol Water Uptake, *Atmos. Chem. Phys.*, 2013, **13**(2), 717–740, DOI: **10.5194/acp-13-717-2013**.
77 M. Gavish, R. Popovitz-Biro, M. Lahav and L. Leiserowitz, Ice Nucleation by Alcohols Arranged in Monolayers at the Surface of Water Drops, *Science*, 1990, **250**(4983), 973–975, DOI: **10.1126/science.250.4983.973**.
78 P.-B. Ronit, J. L. Wang, J. Majewski, E. Shavit, L. Leiserowitz and M. Lahav, Induced Freezing of Supercooled Water into Ice by Self-Assembled Crystalline Monolayers of Amphiphilic Alcohols at the Air-Water Interface, *J. Am. Chem. Soc.*, 1994, **116**(4), 1179–1191, DOI: **10.1021/ja00083a003**.
79 B. Zobrist, T. Koop, B. P. Luo, C. Marcolli and T. Peter, Heterogeneous Ice Nucleation Rate Coefficient of Water Droplets Coated by a Nonadecanol Monolayer, *J. Phys. Chem. C*, 2007, **111**(5), 2149–2155, DOI: **10.1021/jp066080w**.
80 D. A. Knopf and S. M. Forrester, Freezing of Water and Aqueous NaCl Droplets Coated by Organic Monolayers as a Function of Surfactant Properties and Water Activity, *J. Phys. Chem. A*, 2011, **115**(22), 5579–5591, DOI: **10.1021/jp2014644**.
81 J. Majewski, R. Popovitz-biro, W. G. Bouwman, K. Kjaer, J. Als-nielsen, M. Lahav and L. Leiserowitz, The Structural Properties of Uncompressed Crystalline Monolayers of Alcohols CnH2n+1 OH (N = 13–31) on Water and Their Role as Ice Nucleators, *Chem.–Eur. J.*, 1995, **1**(5), 304–311, DOI: **10.1002/chem.19950010507**.
82 E. Ochshorn and W. Cantrell, Towards Understanding Ice Nucleation by Long Chain Alcohols, *J. Chem. Phys.*, 2006, **124**(5), 1–6, DOI: **10.1063/1.2166368**.
83 Y. Qiu, N. Odendahl, A. Hudait, R. Mason, A. K. Bertram, F. Paesani, P. J. DeMott and V. Molinero, Ice Nucleation Efficiency of Hydroxylated Organic Surfaces Is Controlled by Their Structural Fluctuations and Mismatch to Ice, *J. Am. Chem. Soc.*, 2017, **139**(8), 3052–3064, DOI: **10.1021/JACS.6B12210**.
84 L. H. Seeley and G. T. Seidler, Preactivation in the Nucleation of Ice by Langmuir Films of Aliphatic Alcohols, *J. Chem. Phys.*, 2001, **114**(23), 10464–10470, DOI: **10.1063/1.1375151**.
85 R. J. Perkins, M. G. Vazquez De Vasquez, E. E. Beasley, T. C. J. Hill, E. A. Stone, H. C. Allen and P. J. Demott, Relating Structure and Ice Nucleation of Mixed Surfactant Systems Relevant to Sea Spray Aerosol, *J. Phys. Chem. A*, 2020, **124**(42), 8806–8821, DOI: **10.1021/ACS.JPCA.0C05849/ASSET/IMAGES/LARGE/JP0C05849_0012.JPEG**.
86 T. Koop, Homogeneous Ice Nucleation in Water and Aqueous Solutions, *Z. Phys. Chem.*, 2004, **218**(11–2004), 1231–1258, DOI: **10.1524/zpch.218.11.1231.50812**.
87 G. P. Schill, K. Genareau and M. A. Tolbert, Deposition and Immersion-Mode Nucleation of Ice by Three Distinct Samples of Volcanic Ash, *Atmos. Chem. Phys.*, 2015, **15**(13), 7523–7536, DOI: **10.5194/acp-15-7523-2015**.
88 Y. Tobo, P. J. Demott, T. C. J. Hill, A. J. Prenni and G. D. Franc, Organic Matter Matters for Ice Nuclei of Agricultural Soil Origin, *Atmos. Chem. Phys.*, 2014, **14**(16), 8521–8531, DOI: **10.5194/acp-14-8521-2014**.
89 C. M. Beall, M. D. Stokes, T. C. Hill, P. J. Demott, J. T. Dewald and K. A. Prather, Automation and Heat Transfer Characterization of Immersion Mode Spectroscopy for Analysis of Ice Nucleating Particles, *Atmos. Meas. Tech.*, 2017, **10**(7), 2613–2626, DOI: **10.5194/amt-10-2613-2017**.
90 T. F. Whale, B. J. Murray, D. O. Sullivan, T. W. Wilson, N. S. Umo, K. J. Baustian and J. D. Atkinson, A Technique for Quantifying Heterogeneous Ice Nucleation in Microlitre Supercooled Water Droplets, *Atmos. Meas. Tech.*, 2015, **8**(6), 2437–2447, DOI: **10.5194/amt-8-2437-2015**.
91 B. J. Murray, S. L. Broadley, T. W. Wilson, J. D. Atkinson and R. H. Wills, Heterogeneous Freezing of Water Droplets Containing Kaolinite Particles, *Atmos. Chem. Phys.*, 2011, **11**(9), 4191–4207, DOI: **10.5194/acp-11-4191-2011**.
92 S. Kasparoglu, R. Perkins, P. J. Ziemann and P. J. Demott, Experimental Determination of the Relationship Between Organic Aerosol Viscosity and Ice Nucleation at Upper Free Tropospheric Conditions, *J. Geophys. Res.: Atmos.*, 2022, **127**(16), 1–20, DOI: **10.1029/2021JD036296**.
93 B. Wang, A. T. Lambe, P. Massoli, T. B. Onasch, P. Davidovits, D. R. Worsnop and D. A. Knopf, The Deposition Ice Nucleation and Immersion Freezing Potential of Amorphous Secondary Organic Aerosol : Pathways for Ice and Mixed-Phase Cloud Formation, *J. Geophys. Res.: Atmos.*, 2012, **117**(D16), 1–12, DOI: **10.1029/2012JD018063**.
94 B. J. Murray, T. W. Wilson, S. Dobbie, Z. Cui, S. M. R. K. Al-Jumur, O. Möhler, M. Schnaiter, R. Wagner, S. Benz, M. Niemand, H. Saathoff, V. Ebert, S. Wagner and

B. Kärcher, Heterogeneous Nucleation of Ice Particles on Glassy Aerosols under Cirrus Conditions, *Nat. Geosci.*, 2010, **3**(4), 233–237, DOI: **10.1038/ngeo817**.

95 T. W. Wilson, B. J. Murray, R. Wagner, O. Möhler, H. Saathoff, M. Schnaiter, J. Skrotzki, H. C. Price, T. L. Malkin, S. Dobbie and S. M. R. K. Al-Jumur, Glassy Aerosols with a Range of Compositions Nucleate Ice Heterogeneously at Cirrus Temperatures, *Atmos. Chem. Phys.*, 2012, **12**(18), 8611–8632, DOI: **10.5194/acp-12-8611-2012**.

96 K. Fowler, P. Connolly and D. Topping, Modelling the Effect of Condensed-Phase Diffusion on the Homogeneous Nucleation of Ice in Ultra-Viscous Particles, *Atmos. Chem. Phys.*, 2020, **20**(2), 683–698, DOI: **10.5194/acp-20-683-2020**.

97 T. Berkemeier, M. Shiraiwa, U. Pöschl and T. Koop, Competition between Water Uptake and Ice Nucleation by Glassy Organic Aerosol Particles, *Atmos. Chem. Phys.*, 2014, **14**(22), 12513–12531, DOI: **10.5194/acp-14-12513-2014**.

98 G. P. Schill and M. A. Tolbert, Heterogeneous Ice Nucleation on Simulated Sea-Spray Aerosol, *J. Phys. Chem. C*, 2014, **118**(50), 29234–29241, DOI: **10.1021/jp505379j**.

99 T. P. Wright and M. D. Petters, The Role of Time in Heterogeneous Freezing Nucleation, *J. Geophys. Res.: Atmos.*, 2013, **118**(9), 3731–3743, DOI: **10.1002/jgrd.50365**.

100 P. J. Demott, R. H. Mason, C. S. Mccluskey, T. C. J. Hill, R. J. Perkins, Y. Desyaterik, A. K. Bertram, J. V. Trueblood, V. H. Grassian, Y. Qiu, V. Molinero, Y. Tobo, C. M. Sultana, C. Lee and K. A. Prather, Ice Nucleation by Particles Containing Long-Chain Fatty Acids of Relevance to Freezing by Sea Spray Aerosols, *Environ. Sci.: Processes Impacts*, 2018, **20**(11), 1559–1569, DOI: **10.1039/c8em00386f**.

101 S. R. Suda, M. D. Petters, G. K. Yeh, C. Strollo, A. Matsunaga, A. Faulhaber, P. J. Ziemann, A. J. Prenni, C. M. Carrico, R. C. Sullivan and S. M. Kreidenweis, Influence of Functional Groups on Organic Aerosol Cloud Condensation Nucleus Activity, *Environ. Sci. Technol.*, 2014, **48**(17), 10182–10190, DOI: **10.1021/es502147y**.

102 P. Bieber and N. Borduas-Dedekind, High-Speed Cryo-Microscopy Reveals That Ice-Nucleating Proteins of Pseudomonas Syringae Trigger Freezing at Hydrophobic Interfaces, *Sci. Adv.*, 2024, **10**(27), 1–11, DOI: **10.1126/sciadv.adn6606**.

103 S. I. Christensen and M. D. Petters, The Role of Temperature in Cloud Droplet Activation, *J. Phys. Chem. A*, 2012, **116**(39), 9706–9717, DOI: **10.1021/jp3064454**.

104 P. R. Tumminello, R. C. James, S. Kruse, A. Kawasaki, A. Cooper, I. Guadalupe-diaz, K. L. Zepeda, D. R. Crocker, K. J. Mayer, J. S. Sauer, C. Lee, K. A. Prather and J. H. Slade, Evolution of Sea Spray Aerosol Particle Phase State Across a Phytoplankton Bloom, *ACS Earth Space Chem.*, 2021, **5**(11), 2995–3007, DOI: **10.1021/acsearthspacechem.1c00186**.

105 E. K. Wilbourn, D. C. O. Thornton, C. Ott, J. Graff, P. K. Quinn, T. S. Bates, R. Betha, L. M. Russell, M. J. Behrenfeld and S. D. Brooks, Ice Nucleation by Marine Aerosols Over the North Atlantic Ocean in Late Spring, *J. Geophys. Res.: Atmos.*, 2020, **125**(4), 1–17, DOI: **10.1029/2019JD030913**.